Shock-Induced Texture in Lunar Mg-Suite Apatite and its Effect on Volatile Distribution

Conference or Workshop Item

SHOCK-INDUCED TEXTURE IN LUNAR MG-SUITE APATITE AND ITS EFFECT ON VOLATILE DISTRIBUTION. A. Cernok[1], J. Darling[2], L. White[2], J.Dunlop[2], and M. Anand[1,3]. [1]Open University, School of Planetary Sciences, Walton Hall, MK7 6AA, United Kingdom (ana.cernok@open.ac.uk), [2]University of Portsmouth, School of Earth & Environmental Sciences, Burnaby Road Portsmouth, PO1 3QL, United Kingdom; [3]Department of Earth Sciences, The Natural History Museum, London, SW7 5BD, UK.

Introduction: The lunar Mg-suite are plutonic rocks which represent an episode of crustal building following primordial differentiation of the Moon [e.g. 1]. They range in crystallization ages from 4.43-4.1 Ga [2]. This suite of rocks includes dunites, troctolites, and norites and comprises 20-30% of the lunar crust up to a depth of ~ 50-60 km. Apatite is the most common volatile-bearing mineral in lunar rocks, which made them an ideal target for *in-situ* studies of volatiles [summarized in 3]. This study focusses on pristine highland samples that have experienced different levels of shock metamorphism [4]. Therefore, they are valuable samples for understanding how the content of water and other volatiles, as well as their isotopic signature respond to shock.

Samples: We studied two highly shocked norites, 78235 & 78236 [5]. These coarse grained cumulate rocks are comprised of ~ 30 % orthopyroxene, ~ 55% Ca-rich plagioclase and maskelynite, ~ 15 % glass and traces of SiO_2 minerals, clinopyroxene, Fe-metal, torilite, Cl-rich fluorapatite, merrillite, baddeleyite, chromite, and Nb-rutile [e.g. 6]. In polished sections these samples display variety of shock-induced features: melt veins, vesicles, maskelynite, heavy fracturing of minerals and wavy extinction. This study builds on the previous work [7, 8] which reported H_2O, Cl, δD and $\delta^{37}Cl$ composition of apatite from these rocks. Two apatites within 78236 (Ap1 and Ap5) contain very different water contents (~200-300 ppm vs. 550-1600 ppm), while the second grain also shows high intra-granular inhomogeneity (Fig. 1). δD values between the grains do not show such high discrepancies: δD= +157 ± 163 ‰ to +196 ± 240 ‰. So far, no satisfactory explanation as to how these discrepancies in water content arose has emerged. Our integrated *EBSD, CL and Raman* analyses have revealed important features which may help address these inhomogeneities.

Analytical procedure: This study represents an integrated analyses of petrographic context and internal texture of apatite combined with previously reported *in-situ* volatile content and isotopic measurements. The search for apatite grains within thin-section was performed using the EDS elemental X-ray mapping procedure using a Secondary Electron Microscope (SEM). The petrographic context was evaluated by EDS-spot analyses of the minerals surrounding apatite. Cathodoluminescence (CL) detector mounted on a SEM was used to investigate homogeneity or internal zoning of selected apatite grains. Phase identification and distribution was carried out by Raman spectroscopy. Lattice orientation and internal structural disorder of selected apatites was studied by Electron Backscatter Diffraction (EBSD). We plan to analyse the sample 78236 by NanoSIMS, to understand if apatites within this similar rock display comparably similar H_2O and δD signatures to that of 78235.

Results: *EDS* mapping revealed ~ 10 apatites in each thin-section which have lengths greater than 5 µm, the largest grain having a surface area of ~ 50 x 15 μm^2. All apatites have anhedral grain shape, mostly showing sub-equant crystal habit. Apatite is found in association with 1) predominantly plagioclase/maskelynite; 2) predominantly Opx, 3) equally associated with different minerals (plagioclase, Opx, Cpx, silica, merrillite).

EBSD scanning across different apatites revealed that those grains entirely surrounded by plagioclase/maskelynite mostly show very weak or no diffraction, appearing quasi-amorphous. Detailed (300 nm step-size) analyses of selected well-diffracting

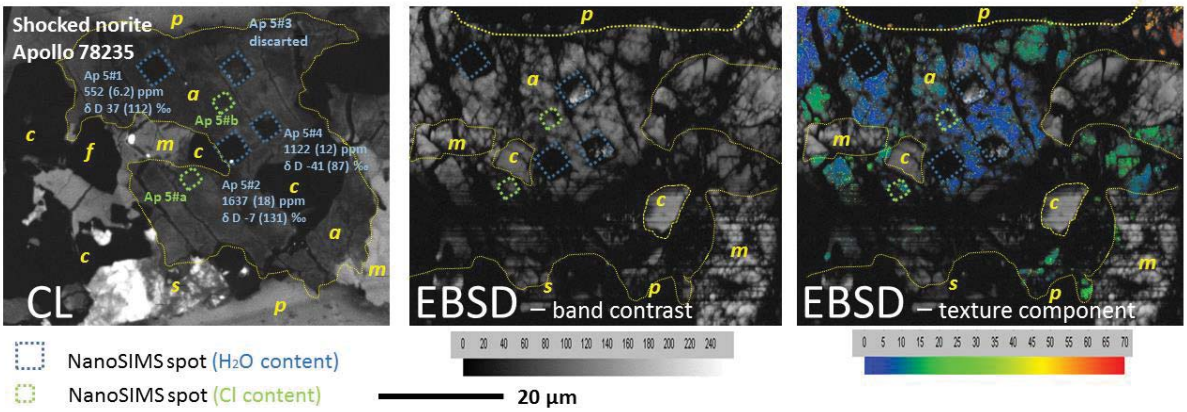

Figure 1. CL, EBSD band contrast and texture component map of apatite (Ap5) in 78235. Yellow dashed line outlines the grain boundary of apatite (a); c-cpx, f – iron, m – merrillite, s – silica, p – plagioclase. CL picture is slightly zoomed out.

apatites indicated degraded crystallinity, as expressed by very low band contrast (BC) values (< 40) (Fig. 1). BC is a quality factor that describes the average intensity of the Kikuchi bands with respect to the overall intensity within the Electron Backscatter Pattern. Internal structure of those grains is highly fractured and segmented, with variable size of fragments among different apatites, as well as within individual grains. Based on the texture component maps, we conclude that no recrystallization of apatite had taken place and that the individual segments within single grains are similarly oriented. However, continuous gradients in texture component map show up 25º of misorientation within single grain, an evidence for severe crystal-plastic deformation. The effect of shock impedance of the major minerals on the associated accessory phases was seen for other minor minerals, e.g. baddeleyite [9].

CL imaging of apatites indicated no complex zoning. Simple, cloudy textures recognized in several grains can be related to the regions of poor crystallinity revealed by EBSD. An example of irregular cloudy zoning is seen for Ap5 in Figure 1. The regions which appear brighter in CL, corresponding to darker, more degraded regions of BC but also follow the set of cracks which are pervasive through the whole grain.

In-situ Raman spectroscopy. Detailed 2D Raman maps of Ap1 revealed very fine-scaled, sub-µm intergrowth of apatite and associated Opx (Fig. 2). The entire region of apatite close to the Opx inclusions shows mixed Raman signal of apatite and Opx (Fig. 2). This region also showed mixed composition in EDS, brighter cloudy zoning in CL, as well as the most degraded crystallinity in BC. Associated with this region is a NanoSIMS spot of lower water content (~200 ppm). According to the imaging, this region of apatite has experienced more intense distortion than the unmixed region of the same grain. However, a slight decrease in water content cannot be attributed to the impact devolatilization, as it may be associated with the fine-grained intergrowth with Opx, which contains less water than apatite. The curious intergrowth of apatite with Opx was described much earlier [6] but to our knowledge it has not been studied in more detail since.

Ap5 grain is closely related to Cpx (augite composition), plagioclase (anorthitic), merrillite, iron and silica (Fig. 1). Here we observe the opposite – the region of apatite further from the Cpx contains less water (~ 500 ppm); the region close to the Cpx, which appears less crystalline, is more water rich (~ 1600 ppm). The region in Ap5 which is Cpx-free, but shows the same CL zoning and low BC contrast due to severe structural distortion, also contains higher water content (~ 1200 ppm, Ap5#4 in Fig. 2). We do not find evidence for Cpx fine-intergrowth with apatite. The results suggest that the late-stage apatite crystallized alongside silica and Cpx in an Opx-free assemblage contain more water than the apatite associated with Opx. The Ap5 shows higher water content in regions which show lowest crystallinity, suggesting enrichment through an impact. We are currently studying other highland samples to confirm this observation.

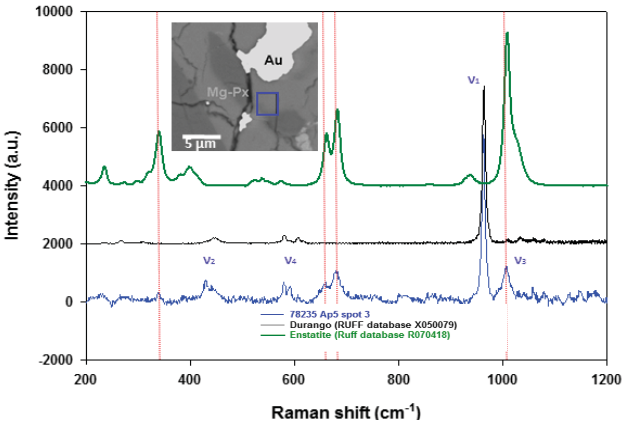

Figure 2. Selected Raman spectrum of Ap1 in 78235 (blue), compared to database. The spectrum shows a mixed phase of apatite and Opx collected within the blue square presented on the inset BSE image, compared to enstatite spectrum (green). Au is a gold-filled NanoSIMS pit. Other minor phases (< 5 µm length) in contact with apatite are Cr-spinel, CPX, and silica.

On most of the remaining apatites, Raman spectra was acquired by spot analyses. Unlike EBSD, Raman has not revealed entirely amorphous apatites. Acquired spectra show good crystallinity also in regions which appear poorly crystallized in BC (e.g. spectrum in Fig. 2). The apatites surrounded by plagioclase or maskelynite, which show the most degraded crystallinity among all apatites studied, show Raman spectra of decreased quality – low signal to noise ratio, less intense peaks and slight peak broadening, but can be easily assigned to apatite. We believe that Raman and EBSD show complementary results. Interaction volume of Raman analysis (1-2 µm) is greater than that of EBSD (few tens of nm), and therefore samples a mixture of sub-micron crystallites surrounded by amorphous medium. EBSD, on the contrary, is very site-specific and sets constraints on the size of crystallites to less than the step size of analyses (300 nm). Additional TEM work is needed to address the crystallinity issue properly, but a recent study [9] has made similar observations in case of baddeleyite.

Acknowledgements: We thank NASA CAPTEM for allocation of lunar samples. AC thanks European Commission for a Marie Curie Fellowship. This research was partially supported by a STFC grant to MA (grant # ST/L000776/1-Project N).

References: [1] Papike J. J. et al. (1996) *GCA, 60,* 3967–3978. [2] Shearer C.K. at al. (2015) *AM*, 100, 294-325. [3] McCubbin F.M. et al. (2015) *AM, 100,* 1668-1707. [4] Warren P.H. (1993) *AM*, 78, 360-376. [5] Jackson E.D. et al. (1975), *Geol.Soc.Am.Bull*. 86, 433-442. [6] Steele I.M. (1975), *AM*, 60, 1086-1091. [7] Barnes J.J. et al. (2014), *EPSL*, 390, 244-252. [8] Barnes J.J. et al. (2016), *EPSL*, 447, 84–94. [9] Darling J. R. et al. (2016), EPSL, 444, 1-12.